Aspirin-triggered 15-Epi-Lipoxin A_4 (LXA_4) and LXA_4 Stable Analogues Are Potent Inhibitors of Acute Inflammation: Evidence for Anti-inflammatory Receptors

By Tomoko Takano,*‡ Stefano Fiore,* Jane F. Maddox,* Hugh R. Brady,‡ Nicos A. Petasis,§ and Charles N. Serhan*

*From the *Center for Experimental Therapeutics and Reperfusion Injury, Department of Anesthesia, and the ‡Renal Division, Department of Medicine, Brigham and Women's Hospital, Harvard Medical School, Boston, Massachusetts 02115; and the §Department of Chemistry, University of Southern California, Los Angeles, California 90089*

Summary

Lipoxins are bioactive eicosanoids that are immunomodulators. In human myeloid cells, lipoxin (LX) A_4 actions are mediated by interaction with a G protein–coupled receptor. To explore functions of LXA_4 and aspirin-triggered 5(*S*),6(*R*),15(*R*)-trihydroxy-7,9,13-*trans*-11-*cis*–eicosatetraenoic acid (15-epi-LXA_4) in vivo, we cloned and characterized a mouse LXA_4 receptor (LXA_4R). When expressed in Chinese hamster ovary cells, the mouse LXA_4R showed specific binding to [^{3}H]LXA_4 ($K_d \approx 1.5$ nM), and with LXA_4 activated GTP hydrolysis. Mouse LXA_4R mRNA was most abundant in neutrophils. In addition to LXA_4 and 15-epi-LXA_4, bioactive LX stable analogues competed with both [^{3}H]LXA_4 and [^{3}H]leukotriene D_4 (LTD_4)–specific binding in vitro to neutrophils and endothelial cells, respectively. Topical application of LXA_4 analogues and novel aspirin-triggered 15-epi-LXA_4 stable analogues to mouse ears markedly inhibited neutrophil infiltration in vivo as assessed by both light microscopy and reduced myeloperoxidase activity in skin biopsies. The 15(*R*)-16-phenoxy-17,18, 19,20-tetranor-LXA_4 methyl ester (15-epi-16-phenoxy-LXA_4), an analogue of aspirin triggered 15-epi-LXA_4, and 15(*S*)-16-phenoxy-17,18,19,20-tetranor-LXA_4 methyl ester (16-phenoxy-LXA_4) were each as potent as equimolar applications of the anti-inflammatory, dexamethasone. Thus, we identified murine LXA_4R, which is highly expressed on murine neutrophils, and showed that both LXA_4 and 15-epi-LXA_4 stable analogues inhibit neutrophil infiltration in the mouse ear model of inflammation. These findings provide direct in vivo evidence for an anti-inflammatory action for both aspirin-triggered LXA_4 and LXA_4 stable analogues and their site of action in vivo.

Lipoxins are trihydroxytetraene-containing eicosanoids that are generated within vascular lumen by platelet-leukocyte interactions and transcellular biosynthetic pathways during multicellular responses such as inflammation, atherosclerosis, and thrombosis (as reviewed in reference 1). This branch of the eicosanoid cascade generates specific tetraene-containing products that appear to function as stop signals. In this regard, lipoxins display selective actions on human leukocytes in vitro that include inhibition of (*a*) FMLP and leukotriene B_4 (LTB_4)[1]-induced neutrophil chemotaxis (2), (*b*) FMLP-induced neutrophil transmigration through epithelial cells (3), and (*c*) neutrophil adhesion and transmigration with endothelial cells (4). We have recently shown that these actions of lipoxin (LX) A_4; 5(*S*),6(*R*),15(*S*)-trihydroxy-7,9,13-*trans*-11-*cis*-eicosatetraenoic acid are mediated via signal transduction events initiated by engagement of high-affinity G protein–coupled receptors in human cells (4–6). This includes LXA_4-induced downregulation of CD11b/CD18 in human neutrophils (5), an adhesion molecule that plays an important role in endothelial–leukocyte interactions (7). Although lipoxins do not directly inhibit the generation

This work was presented in part at the American Society of Nephrology, New Orleans, November 1996.

[1]*Abbreviations used in this paper:* CHO, Chinese hamster ovary cell; DPBS, Dulbecco's phosphate-buffered saline; LO, lipoxygenase; LTB_4, leukotriene B_4; LTD_4, leukotriene D_4; lipoxin A_4 (LXA_4), 5(*S*),6(*R*),15(*S*)-trihydroxy-7,9,13-*trans*-11-*cis*-eicosatetraenoic acid; 15-epi-LXA_4, 5(*S*),6(*R*),15(*R*)-trihydroxy-7,9,13-*trans*-11-*cis*-eicosatetraenoic acid; 15(*R/S*)-methyl-LXA_4, 5(*S*),6(*R*), 15(*R/S*)-trihydroxy-15-methyl-7,9,13-*trans*-11-*cis*-eicosatetraenoic acid; 16-phenoxy-LXA_4, 15(*S*)-16-phenoxy-17,18,19,20-tetranor-LXA_4 methyl ester; 15-epi-16-phenoxy-LXA_4, 15(*R*)-16-phenoxy-17,18,19,20-tetranor-LXA_4 methyl ester; 15(*R/S*)-16-phenoxy-11,12-acetylenic-LXA_4, 15(*R/S*)-16-phenoxy-11,12-acetylenic-17,18,19,20-tetranor-LXA_4 methyl ester; LX, lipoxin; MPO, myeloperoxidase; RACE, rapid amplification of cDNA end.

of reactive oxygen species by activated neutrophils (reviewed in reference 8), the ability of LX to block endothelial cell–leukocyte interactions (4) can also prevent injury initiated by leukocyte-derived reactive oxidants (9, 10). Taken together, these results suggest that lipoxins play important regulatory roles in leukocyte trafficking and inflammation.

The biosynthesis of lipoxins is initiated through cell–cell and lipoxygenase (LO) interactions that are regulated by specific cytokines (1). One major pathway is mounted during PMN–platelet interaction and involves both the 5-LO and 12-LO, and the other involves interactions between the 5-LO and 15-LO (recently reviewed in reference 8) that are controlled by the cytokines IL-4 and IL-13 (11). Given the wide use of aspirin, the mechanism of aspirin's beneficial actions in inflammation remains a topic of intense interest. Aspirin has no direct impact on the lipoxygenases (8). In this regard, a third major pathway for lipoxin biosynthesis was recently uncovered, which involves prostaglandin H synthase-II (PGHS-II) in endothelial cells and 5-LO in leukocytes that generate novel 15-epi-lipoxins when PGHS-II is acetylated after treatment with aspirin (12). The aspirin-triggered lipoxins, for example, 5(*S*),6(*R*),15(*R*)-trihydroxy-7,9,13-*trans*-11-*cis*-eicosatetraenoic acid (15-epi-LXA_4), carries its C-15 alcohol in the *R* configuration, instead of *S* as in native LXA_4, and has potent inhibitory actions in neutrophil adhesion, and 15-epi-LXB_4 blocks cell proliferation in vitro (12, 13). This pathway that leads to 15-epi-LXA_4 may mediate, in part, some of the beneficial actions of aspirin.

Lipoxins are also generated in vivo in humans and in experimental animals (reviewed in reference 8). LXA_4 and LXB_4 are both formed in ischemic rat brain (14), and LXA_4 is generated in mouse kidneys with glomerulonephritis in a P-selectin–dependent fashion predominantly via interactions between platelets and neutrophils (15). In rats, the infiltration of neutrophils to glomerulonephritic kidneys is markedly inhibited by prior exposure of neutrophils to LXA_4 (16). Also, LXA_4 has recently been found to regulate LTB_4-mediated delayed hypersensitive reactions in guinea pig (17). The actions of LXA_4 are not mediated by competition at the LTB_4 receptor (18), but LXA_4 is reported to antagonize the formation of intracellular signals such as IP_3 (19). In addition to its selective actions with leukocytes, LXA_4 also modulates the vasoconstrictor actions of leukotriene D_4 (LTD_4) in renal hemodynamics and is vasodilatory (20). These actions of LXA_4 are mediated by a receptor distinct from that of the myeloid LXA_4R and are consistent with LXA_4 acting on a subtype of the peptido-leukotriene receptors, competing for LTC_4 and LTD_4 high-affinity sites that are present on both mesangial (20) and endothelial cells (21). Interest in the actions of LXA_4 is also heightened by findings with human subjects that indicate that LXA_4 administration via inhalation significantly blocks airway constriction in asthmatic subjects (22).

To explore biological functions of both lipoxins and the recently identified aspirin-triggered lipoxins in vivo, it is essential to identify the molecular basis of their response in experimental animals. To this end, we report here isolation of the mouse lipoxin A_4 receptor (LXA_4R) and that stable analogues of LXA_4 and the aspirin-triggered 15-epi-LXA_4 that specifically compete at this site are potent inhibitors of acute neutrophil infiltration in vivo.

Materials and Methods

Materials. Tritiated LXA_4 ([11,12-^{3}H]LXA_4; ~40 Ci/mmol) was obtained by custom catalytic hydrogenation of 11,12-acetylenic-LXA_4 methyl ester that was supplied to and performed at Du Pont New England Nuclear (Boston, MA), and the labeled LXA_4 was purified as in Fiore et al. (18). α-[^{32}P]dCTP (3,000 Ci/mmol) and γ-[^{32}P]GTP (30 Ci/mmol) were purchased from Du Pont NEN. LXA_4 synthetic analogues, 15-epi-LXA_4-methyl ester, 5(*S*),6(*R*),15(*R*/*S*)-trihydroxy-15-methyl-7,9,13-*trans*-11-*cis*-eicosatetraenoic acid (15[*R*/*S*]-methyl-LXA_4) methyl ester, and 16-phenoxy-17,18,19,20-tetranor-LXA_4-methyl ester, were prepared, isolated and analyzed as described (23). 15(*R*)-16-phenoxy-17,18,19,20-tetranor-LXA_4 methyl ester (15-epi-16-phenoxy-LXA_4) and 15(*R*/*S*)-16-phenoxy-11,12-acetylenic-17,18,19,20-tetranor-LXA_4 methyl ester (15[*R*/*S*]-16-phenoxy-11,12-acetylenic-LXA_4) as methyl esters were designed from knowledge of 15-epi-LXA_4 structure and bioactivities (12) and were separated and isolated by RP-HPLC, and their identities were confirmed by NMR. Synthetic LXB_4, LTB_4, and LTD_4 were obtained from Cascade Biochem Ltd. (Reading, Berkshire, England). SKF-104353 was a gift from Smith Kline and French Laboratories (King of Prussia, PA). Dulbecco's phosphate-buffered saline (DPBS) and cell culture reagents were from Whittaker M.A. Bioproducts (Walkersville, MD). Casein was from Sigma Chemical Co. (St. Louis, MO), and silicon oil was from Hüls America (Bristol, PA). Balb/c mice were purchased from Jackson Laboratory (Bar Harbor, ME).

cDNA Cloning of Mouse LXA_4 Receptor. A mouse spleen cDNA library was purchased from Clontech (Palo Alto, CA), and 6×10^5 clones were screened with the EcoRI fragment from the human LXA_4R cDNA employing high stringency. A positive clone (designated 15-2) was isolated. Phage DNA was amplified and purified, and the insert cDNA was excised by EcoRI digestion and subcloned into the EcoRI site of pBluescript II KS(+) (obtained from Stratagene, La Jolla, CA). Sequence analysis showed that this clone 15-2 was a partial clone lacking the amino terminal region (nucleotide 87, of full-length clone; see Fig. 1). To obtain the missing amino-terminal region, we used the rapid amplification of cDNA end or rapid amplification of cDNA end (RACE) technique. The 5′-RACE-Ready cDNA™ from spleen was purchased from Clontech (Palo Alto, CA), and RACE was performed according to the manufacturer's instructions. The first round of PCR was done between the anchor primer provided by the manufacturer and synthetic primer 5′-GCCATTTCAACAAGAAG-GAATGGTAGAG-3′ (antisense of nucleotide 229–257) for 30 cycles (94°C for 30 s, 60°C for 45 s, 72°C for 2 min). The first PCR product was diluted to 1:50, and a second round of PCR was carried out between the anchor primer and a synthetic primer 5′-GCTGTGAAAGAGAAGTCAGCCAATGCTA-3′ (antisense of nucleotide 199–227) using the same condition for 35 cycles. A PCR product of ~300 bp was obtained and subcloned into pBluescript II KS(+) for sequencing. Overlapping regions of RACE product and clone 15-2 (nucleotide 87–198) were found to be identical. The RACE product was subcloned to the 5′ end

of clone 15-2 to construct a full-length clone, using a SpeI site at nucleotide 136. Hydrophobicity analysis of amino acid sequence and homology comparison were performed using Lasergene (DNASTAR Inc., Madison WI).

Confirmation of the Mouse PMN Receptor Sequence. The sequence of the murine LXA_4R clone from the spleen library was confirmed by RT-PCR of RNA obtained from isolated mouse neutrophils. In brief, for isolation of mouse neutrophils, 2 ml of 2% casein solution was injected into the peritoneal cavity of 8-wk-old female Balb/c mice. 4 h later, peritoneal lavages were performed with $DPBS^{2+}$. Wright-Giemsa staining and light microscopy showed that ~85% of the cells harvested were neutrophils, which were next taken for centrifugation and extraction of RNA using TriZol reagent (GIBCO BRL, Gaithersburg, MD) following manufacturer's instructions. 0.5 μg RNA was reverse-transcribed and used as the template for PCR, which was performed with sense primer 5′-CAGCTGGTTGTGCAGACAAAATG-3′ (corresponding to nucleotide −20 to 3) and antisense primer 5′-CATCCCA-CAGCCCCCTCCTCA-3′ (corresponding to nucleotide 1054–1074), for 25 cycles (94°C for 30 s, 64°C for 45 s, 72°C for 80 s). The PCR product was subcloned into pBluescript II KS(+) and five isolated independent clones were sequenced for confirmation; each was found to be identical.

Binding Characteristics of [^{3}H]LXA_4 to Chinese Hamster Ovary Cells Transfected with Mouse LXA_4R cDNA. The coding region of mouse LXA_4R was subcloned into mammalian expression vector pcDNA3 (Invitrogen, San Diego, CA). This plasmid was transfected into Chinese hamster ovary (CHO) cells by the DEAE-dextran method, and after 48 h a binding experiment of [^{3}H]LXA_4 was performed as in Fiore et al. (6). Cells were harvested in $DPBS^{2-}$ (5 mM EDTA), washed twice in $DPBS^{2+}$, and adjusted to 10^6 cells/ml. For time course experiments, cells were incubated with 0.3 nM of [^{3}H]LXA_4 in the presence or absence of 300 nM unlabeled LXA_4 at 4°C for the indicated times. For further analysis, cells were incubated with 0.3 nM of [^{3}H]LXA_4 in the presence of increasing concentrations of the homoligand LXA_4 for 5 min. Reactions were terminated by rapid centrifugation (12,000 *g*, 60 s) through silicon oil ($d = 1.028$), and cell-associated radioactivity was determined by liquid scintillation counting. Specific binding was obtained by subtracting nonspecific binding in the presence of 3 log order excess of unlabeled LXA_4 from each count, and 10^6 cells were used per each point. Data were analyzed with the Ligand program (Biosoft Elsevier, Cambridge, U.K.).

Establishment of Stable Transformant of the Mouse LXA_4R. Mouse LXA_4R cDNA in mammalian expression vector pcDNA3 was also used to establish a CHO cell line stably expressing the mouse LXA_4R (i.e., mouse LXA_4R stable transformant). Mouse LXA_4R cDNA and vector alone, namely, pcDNA3 (used as a mock control), were transfected into CHO-K1 cells by electroporation, and transformants were selected under the existence of 1g/l G418 for ~2 wk. Expression levels of mouse LXA_4R mRNA of individual colonies were examined by northern hybridization, using mouse LXA_4R cDNA as a probe.

Ligand Operated Guanosine Triphosphate. Guanosine triphosphate activity was determined in mouse LXA_4R stable transformant as in Fiore et al. (6) with slight modification. Reactions were terminated at 3 min and the rate of GTP hydrolysis was calculated between time zero and 3 min.

Northern Hybridization of Mouse and Human Multiple Tissue Blot. Mouse Multiple Tissue Northern Blot™ including 2 μg each poly(A)$^+$ RNA of heart, brain, spleen, lung, liver, skeletal muscle, kidney, and testis was purchased from Clontech (Palo Alto, CA). Mouse neutrophils were isolated by casein-induced peritonitis, as described in "Confirmation of the mouse PMN receptor sequence" (above). Cells were then pelleted by centrifuge, and RNA was extracted using TriZol reagent (GIBCO BRL) following manufacturer's instructions. 10 μg total RNA was separated by gel electrophoresis in 1% agarose gel containing 1.9% formaldehyde and blotted to nylon membrane. BamHI–PstI fragment of mouse LXA_4 receptor (nucleotide 78–966) was labeled with α-[^{32}P]dCTP using an oligolabeling kit (Pharmacia, Piscataway, NJ), and hybridization was performed following the protocol of Church and Gilbert in 1% BSA, 7% SDS, 0.5 M phosphate buffer (pH 6.8), 1 mM EDTA (24), followed by washing in wash buffer A (0.5% BSA, 5% SDS, 40 mM phosphate buffer, pH 6.8, 1 mM EDTA) twice for 20 min at 65°C, and then in wash buffer B (1% SDS, 40 mM phosphate buffer, pH 6.8, 1 mM EDTA) four times for 20 min at 65°C. Filters were exposed to x-ray film with intensifying screen at −70°C for 72 h (neutrophil) or 120 h (multiple tissue blot). The human multiple tissue blot was also purchased from Clontech, and northern hybridization was performed as with mouse, using EcoRI fragment of human LXA_4R cDNA as a probe, and exposed to the x-ray film for 24 h.

Competitive Displacement of [^{3}H]LXA_4 and [^{3}H]LTD_4 Binding by 15-epi-LXA_4 and LXA_4 Analogues. Human PMN were isolated by dextran sedimentation followed by Ficoll gradient separation, and resuspended in $DPBS^{2+}$ (20×10^6/ml) as in Fiore et al. (18). Human umbilical endothelial cells (HUVEC) were cultured in a gelatin-coated (1%) 12-well plate (3.5×10^5/well). PMN and HUVEC were incubated with [^{3}H]LXA_4 (0.3 nM, 5 min at 4°C) and [^{3}H]LTD_4 (5 nM, 90 min at 4°C), respectively, in the presence or absence of the increasing concentrations of LXA_4 (3–300 nM), LTD_4 (5–500 nM) and the indicated LXA_4 analogues (20–2,000 nM). After incubations, cell associated label was separated from free label by silicon oil method (PMN, see above) or washing (HUVEC) as in Fiore et al. (18).

Ear Inflammation Model. Ear inflammation was induced as described by Ekerdt and Müller (25) with the following minor modifications. Balb/c mice (8–10 wk old, female) were anesthetized with intraperitoneal injection of pentobarbital (60 mg/kg). 20 μl of acetone was applied to the inner side of the right ear, and indicated amount of each test compound (i.e., LXA_4 analogues or dexamethasone) suspended in 20 μl acetone was applied to the inner side of the left ear. Approximately 7 min later, LTB_4 (5 μg in 20 μl of acetone) was applied to both ears. At the indicated times, mice were euthanized with an overdose of pentobarbital, and a 6-mm diam of ear sample was obtained from each ear using a skin biopsy punch. Ear skin samples were used for myeloperoxidase assay following the method of Bradley et al. (26). In brief, samples were homogenized in potassium phosphate buffer (pH 6.0) containing 0.5% hexadecyltrimethylammonium bromide, sonicated, and freeze-thawed three times, after which sonication was repeated. The suspension was centrifuged at 16,000 *g* for 20 min, and 100 μl of supernatant was added to 900 μl of potassium phosphate buffer (pH 6.0) containing 0.167 mg/ml *o*-dianisidine dihydrochloride (Sigma) and 0.0006% hydrogen peroxide (American Bioanalytical, Natick, MA). Changes in OD were monitored at 460 nm at 25°C, at 30- and 90-s intervals. Isolated mouse neutrophils obtained from casein-induced peritonitis (as in preceding sections) were processed in the same manner and used to obtain a calibration curve for neutrophils, which were enumerated by light microscopy.

Histological Evaluation of Mouse Ear Skin. Skin samples were obtained using a skin biopsy punch and fixed in 10% buffered formaldehyde. Samples were then paraffin-embedded, sliced, and stained with hematoxylin-eosin.

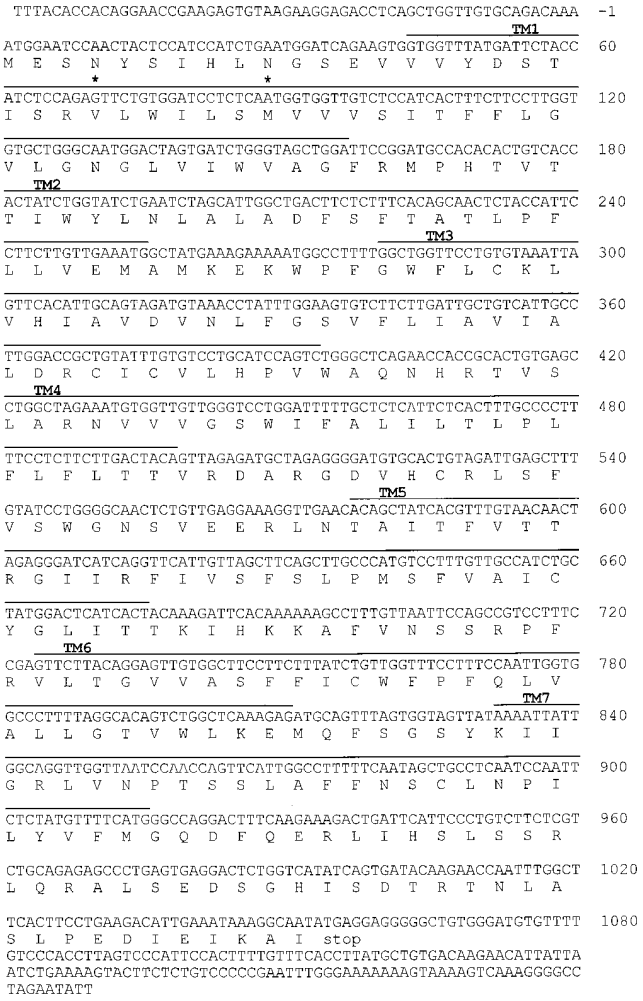

Figure 1. Nucleotide and deduced amino acid sequence of the mouse LXA_4R. The mouse LXA_4R has an open reading frame encoding 351 amino acids. Putative transmembrane regions (TM) are indicated with bars, and possible N-glycosylation sites are indicated by an asterisk (*). These sequence data are available from EMBL/GenBank/DDBJ under the accession number U78299.

Statistical Analysis. Statistical analysis was performed using the Student's *t*-test.

Results

Cloning of the Mouse LXA_4R. To evaluate the role and actions of LX and aspirin-triggered LX stable analogues in vivo, we first sought the identification and distribution of the murine LXA_4 receptor. The mouse LXA_4 receptor was obtained from a mouse spleen cDNA library. Since this initial clone lacked the amino terminus, a full-length clone was obtained using rapid amplification of cDNA end (RACE) technique (see Materials and Methods). The resulting full-length clone had an open reading frame encoding 351 amino acids (Fig. 1). To confirm this clone obtained by the RACE technique, we amplified the coding region of mouse LXA_4R by RT-PCR from RNA obtained from isolated mouse neutrophils. When the PCR product was sequenced,

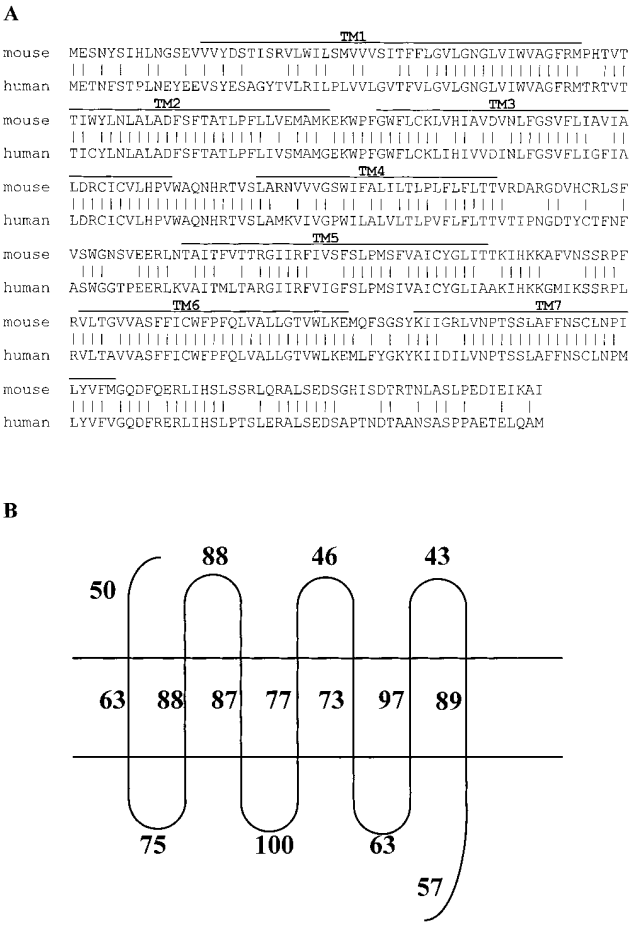

Figure 2. Alignment of human and mouse LXA_4R. (*A*) The amino acid sequence of human LXA_4R was aligned to the mouse homologue. Their amino acid sequences were 73% identical. The vertical bars indicate the identical residues. (*B*) Percentage of identity of each segment is shown.

five independent clones were obtained that were each identical to the clone isolated from spleen. Therefore, we concluded that this LXA_4R cDNA is indeed present not only in the mouse cDNA spleen library, but it is also in mouse neutrophils (see also Fig. 5 *A*).

As expected, hydrophobicity analysis showed the presence of a putative seven transmembrane domain characteristic of the G protein–coupled receptor superfamily (27). The mouse LXA_4R has two N-glycosylation sites in NH_2-terminal extracellular domain, which are also conserved in human LXA_4R (6, 28). The carboxyl-terminal or cytoplasmic tail of the mouse LXA_4R had nine serine or threonine residues, among which six were also conserved in human LXA_4R (Figs. 1 and 2). The overall homology between human and mouse LXA_4Rs was 76% in nucleotide sequence and 73% in the deduced amino acid. An especially high homology was noted in the sixth transmembrane domain and second intracellular loop (Fig. 2), suggesting important roles for these regions in ligand recognition and signal transduction.

Binding Characteristics of Mouse LXA_4R. The human LXA_4R

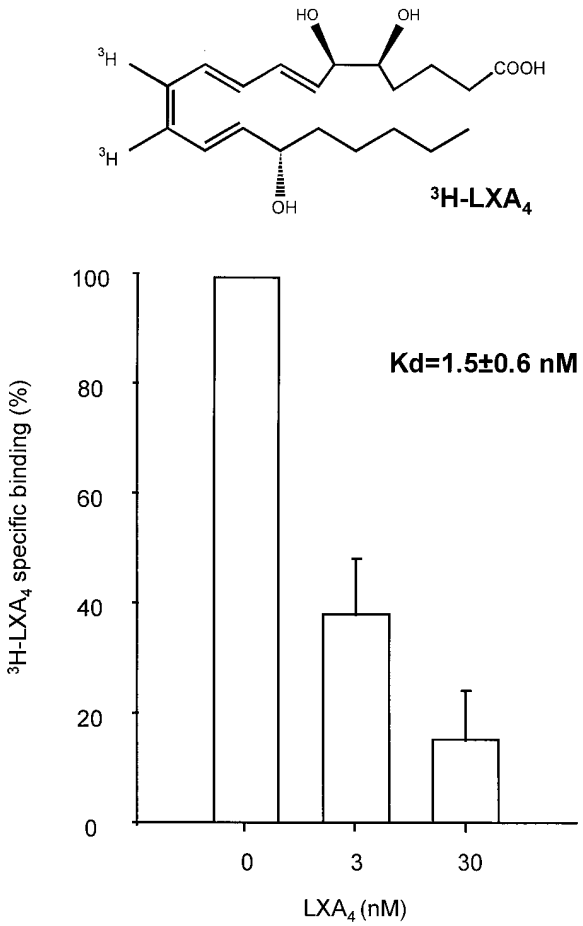

Figure 3. Specific binding characteristics of mouse LXA_4R expressed in CHO cells. After transfection with mouse LXA_4R cDNA (48 h), intact CHO cells were resuspended in $DPBS^{2+}$ (10^6 cells /ml). Cells were incubated with 0.3 nM of [^{3}H]LXA_4 in the presence of indicated concentrations of homoligand for 5 min at 4°C. The incubations were terminated by rapid centrifugation (12,000 *g*, 60 s) through silicon oil ($d = 1.028$), and cell-associated radioactivity was determined with 10^6 cells used per incubation. Data were analyzed with the Ligand program (Biosoft Elsevier). Results are representative of four independent experiments (mean ± SEM, $n = 4$). Specific binding was not detected in the mock transfected cells with vector (pcDNA3) alone.

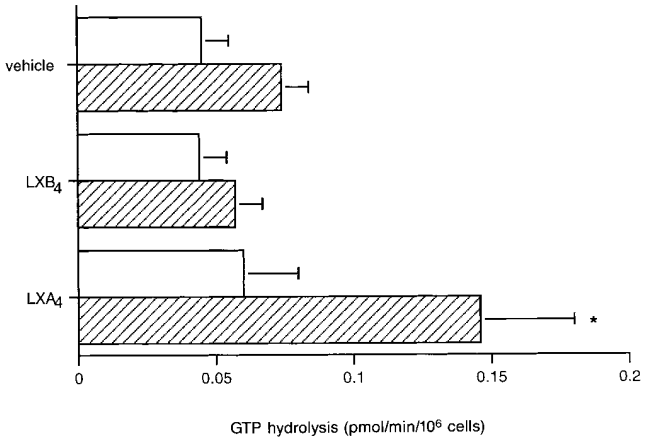

Figure 4. GTP hydrolysis by the mouse LXA_4R stable transformant. Rates of γ-[^{32}P]dCTP hydrolysis were determined by calculating the linear regression of ^{32}Pi release in the initial 3 min after ligand addition (10^{-8} M) to electropermeabilized CHO cells that were stably transfected with mouse LXA_4R cDNA or vector alone. Open bars, mock transfected cells. Hatched bars, mouse LXA_4R stable transformant. Data are mean ± SEM, $n = 4$–5. *$P < 0.05$ to all the other bars.

displays both specific and stereoselective binding and activation with LXA_4, which is ~0.5 nM K_d in human PMN and ~1.7 nM with transfected CHO cells (5, 6, 18). To test the ability of this mouse LXA_4R to bind LXA_4, CHO cells were transfected with mouse LXA_4R cDNA and tested for their ability to specifically bind [^{3}H]LXA_4. Mouse LXA_4R showed specific binding to [^{3}H]LXA_4. When performed at 4°C, the binding saturated after 5 min (data not shown). Scatchard analysis gave a K_d of 1.5 ± 0.6 nM, which was obtained with four separate concentrations of unlabeled LXA_4 (mean ± SEM, $n = 4$), a value similar to that of the human receptor (K_d 1.7 nM) (6), suggesting that this mouse clone encodes the high-affinity LXA_4 receptor (Fig. 3).

Mouse LXA_4R Stable Transformant. Next, we established a stable transformant of the mouse LXA_4R to further evaluate the ability of mouse LXA_4R to transmit signals. One clone (designated P4-5) had the highest mRNA expression of mouse LXA_4R when examined by northern hybridization (data not shown). To test whether this mouse LXA_4R transmits signal when exposed to LXA_4, we examined GTP hydrolysis activity using this stable cell line P4-5. Treatment of CHO cells expressing human LXA_4R with LXA_4 stimulates GTPase activation (see reference 6). Upon exposure to 10^{-8} M LXA_4, the mouse LXA_4R stable transformant activated GTPase approximately twofold when compared to vehicle alone (vehicle 0.07 ± 0.01 vs. LXA_4 0.15 ± 0.03 pmol/min/10^6 cells, mean ± SEM, $n = 5$, $P < 0.05$). This stimulation was stereoselective because, when tested in parallel, equimolar of the positional isomer of LXA_4, LXB_4 did not elicit this activation (vehicle 0.07 ± 0.01 vs. 0.06 ± 0.01 pmol/10^6 cells, mean ± SEM, $n = 5$ and 4, respectively). Mock transfected CHO cells did not respond to LXA_4 (Fig. 4). Thus, we concluded that we have identified a functional LXA_4R of mouse.

Tissue Distribution of Mouse and Human LXA_4R by Northern Hybridization. To obtain the tissue distribution of mouse LXA_4R mRNA, and compare it to that of human, northern hybridization of mouse and human multiple tissue blot was performed (Fig. 5). In mouse, there was one major band of ~1.4 kb with high stringency conditions. LXA_4R mRNA was most abundant in neutrophils, followed by spleen and lung, organs known to carry contaminants for leukocytes (Fig. 5 *A*). When exposed longer (for 14 d), there were faint bands associated with heart and liver (data not shown). In humans, we have previously found that LXA_4R mRNA is abundant in lung tissue (6). In the present experiments, we extended these previous observations and observed that LXA_4R mRNA was also abundant in peripheral leukocytes, followed by spleen (Fig. 5 *B*). In these two organs, in addition to a major band of ~1.4 kb, another band of ~2.4 kb was also observed. In testis, there was a single band of

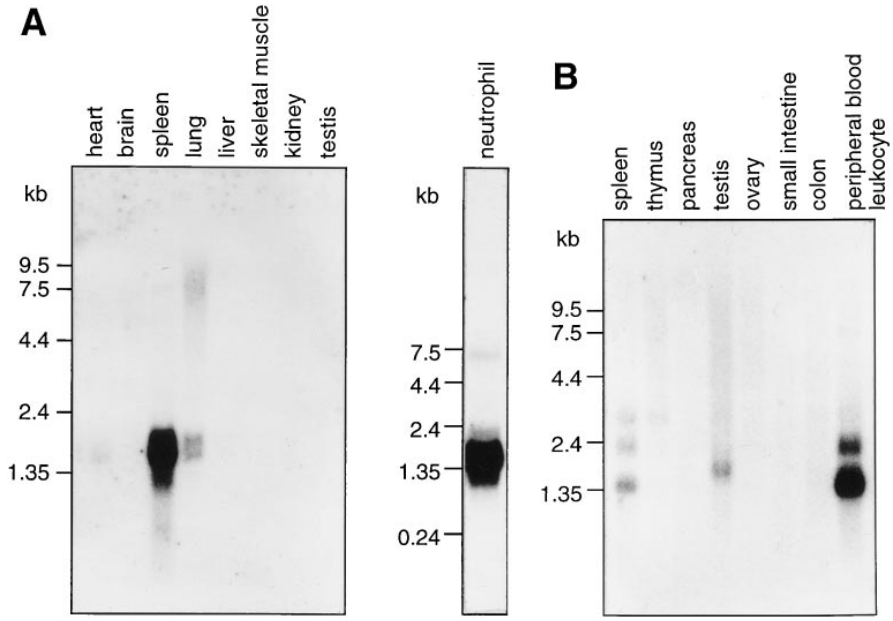

Figure 5. Northern hybridization of the mouse and human LXA_4R. (*A*) Mouse multiple tissue blot: each lane of mouse multiple tissue blot contains 2 μg poly(A)$^+$ RNA. 10 μg of total RNA was used for mouse neutrophil. Filters were hybridized and washed as described in Materials and Methods. Filters were exposed to x-ray film with intensifier at −80°C for 120 h (multiple tissue blot) or 72 h (neutrophil). (*B*) Human multiple tissue blot: each lane contains 2 μg poly(A)$^+$ RNA. Filter was hybridized and washed as described in Materials and Methods. Filter was exposed to x-ray film for 24 h.

∼1.7 kb, which was not present in mouse. These bands of different sizes in human suggest the possibility of alternative splicing in human tissues, but by comparison they are lacking in mouse tissues.

LXA_4 and 15-epi-LXA_4 Stable Analogues Competitively Displace [^{3}H]LXA_4 Binding. Like other autacoids, LXA_4 is rapidly converted within seconds to minutes in the microenvironment to inactive LX metabolites, which involves dehydrogenation at the carbon C-15 position as the predominant route. To evaluate the action of lipoxins in vivo, LXA_4 stable analogues were designed and prepared by total organic synthesis, which resist dehydrogenation and ω-oxidation, and retain bioactivity (23) (Fig. 6). Both 15(*R/S*)-methyl-LXA_4 and 15(*S*)-16-phenoxy-17,18,19, 20-tetranor-LXA_4 methyl ester (16-phenoxy-LXA_4) were more resistant to the dehydrogenation by recombinant 15-hydroxy prostaglandin dehydrogenase (15-PGDH) than LXA_4, and also resistant to conversion by differentiated HL-60 cells, and were potent inhibitors of neutrophil transmigration and adhesion with IC50 ranging from 1–50 nM. 15-epi-LXA_4 (carrying a C-15 alcohol in the *R* configuration), one of the new eicosanoids triggered by aspirin treatment, also displays a slower rate of conversion by recombinant enzyme, suggesting a longer bio-half-life than native LXA_4 with its C-15 alcohol in the *S* configuration.

With these LXA_4 stable analogues in hand, we next examined whether they compete at the same site as native LXA_4 (Fig. 7 *A*). [^{3}H]LXA_4 binds to its specific receptor on human neutrophils (18), and therefore in the present study we used human cells for the purpose of direct comparison with previous findings (Fig. 7 *A*). Moreover, it was not possible to obtain mouse peripheral blood neutrophils in the amounts that would permit specific binding experiments and parallel evaluation of each of the synthetic LX analogues. Each of these bioactive LXA_4 analogues competitively dis-

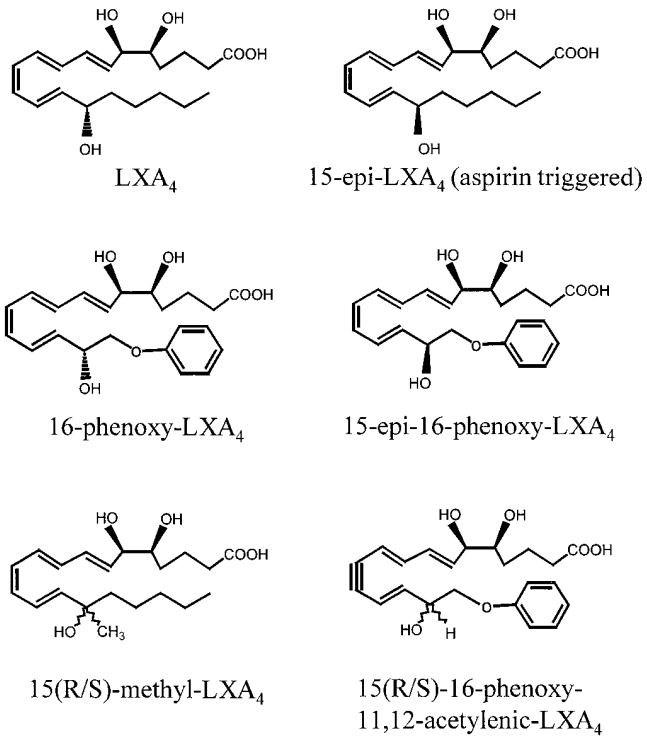

Figure 6. Structure of LXA_4 stable analogues. Structures of LXA_4 stable analogues used in these experiments. 15-epi-LXA_4 is an aspirin triggered lipoxin, and carried a C-15 alcohol at the *R* configuration, opposite to the *S* configuration in native LXA_4. 16-phenoxy-LXA_4 has phenoxy group at C-16, and 15-epi-16-phenoxy-LXA_4 carried its C-15 alcohol at the *R* configuration, in addition to the phenoxy group at C-16, and is a stable analogue of 15-epi-LXA_4. In 15(*R/S*)-methyl-LXA_4, hydrogen at C-15 was replaced by a methyl group as a racemate at C-15. 15(*R/S*)-16-phenoxy-11,12-acetylenic-LXA_4 has a phenoxy group at C-16 and racemic (∼50:50) C-15 alcohol, and also carried an acetylenic bond at C11-12.

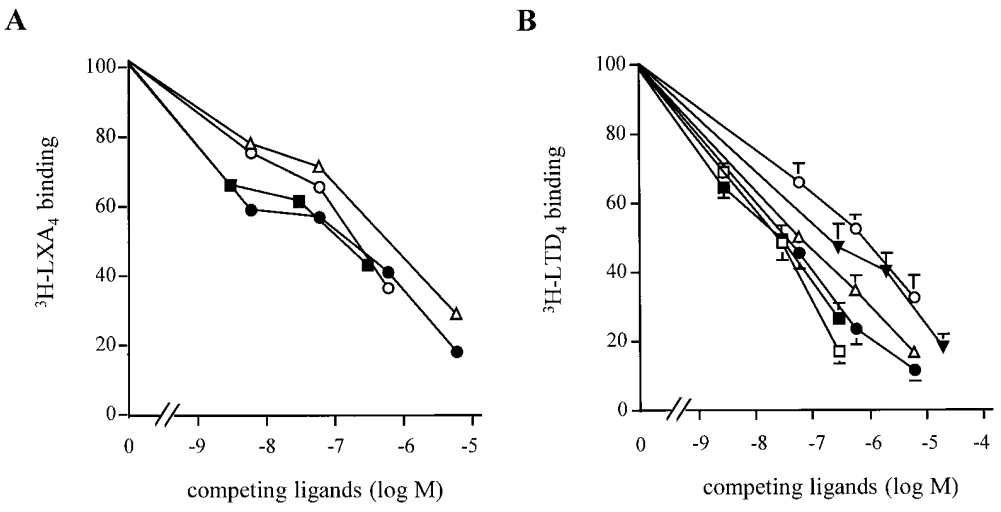

Figure 7. Competitive displacement of [^{3}H]LXA$_4$ and [^{3}H]LTD$_4$ by LXA$_4$ analogues. (*A*) Specific binding of [^{3}H]LXA$_4$ on PMN: comparison of 15(*R*/*S*)-methyl-LXA$_4$, 16-phenoxy-LXA$_4$ and 15-epi-LXA$_4$. PMN were suspended in DPBS (5×10^7cells/ml) and binding of [^{3}H]LXA$_4$ (0.3 nM) was determined at 4°C in the presence or absence of LXA$_4$ (■), 15(*R*/*S*)-methyl-LXA$_4$ (○), 15-epi-LXA$_4$ (●), and 16-phenoxy-LXA$_4$ (△) as described in Materials and Methods. Result is the representative of three independent experiments with duplicate determination. (*B*) Evaluation of LXA$_4$ analogues in [^{3}H]LTD$_4$ displacement assays with HUVEC. Cells were cultured in 12-wells plate ($\sim 3.5 \times 10^5$ cells/well), and [^{3}H]LTD$_4$ (5 nM) binding was assessed at 4°C in the presence or absence of unlabeled LTD$_4$ (□), LXA$_4$(■), 15(*R*/*S*)-methyl-LXA$_4$ (○), 15-epi-LXA$_4$ (●), 16-phenoxy-LXA$_4$ (△) or SKF-104353 (▼) as described in Materials and Methods. Results are the mean ± SEM of three separate experiments with duplicate determinations.

placed [^{3}H]LXA$_4$ binding in the following rank order: homoligand LXA$_4$ ≈ 15-epi-LXA$_4$ >15(*R*/*S*)-methyl-LXA$_4$ >16-phenoxy-LXA$_4$. The K_i values for LXA$_4$ in the present experiments (~2.0 nM) were comparable to the previously reported values for human neutrophils (18) and CHO cells expressing human LXA$_4$R (6). Thus, LXA$_4$ stable analogues compete at the same myeloid receptor as native LXA$_4$ on human PMN.

LXA$_4$ also carries a vasodilatory action, and is known to modulate the specific binding of LTD$_4$ on endothelial cells (21) and glomerular mesangial cells (20). Thus, in addition to acting at the myeloid LXA$_4$R, LXA$_4$ also competes at a receptor subtype that also recognizes and responds to the peptidoleukotriene LTD$_4$. LXA$_4$ also inhibits peptidoleukotriene (LTC$_4$ and LTD$_4$)-induced upregulation of P-selectin in endothelial cells (4). In view of these findings, we examined whether these LXA$_4$ stable analogues could compete for [^{3}H]LTD$_4$–specific binding to endothelial cells. As seen in Fig. 7 *B*, both native LXA$_4$ and 15-epi-LXA$_4$ competed with [^{3}H]LTD$_4$ as effectively as the homoligand LTD$_4$ and the well-characterized LTD$_4$ receptor antagonist SKF-104353. The LX stable analogues 15-(*R*/*S*)-methyl-LXA$_4$ and 16-phenoxy-LXA$_4$ each gave K_i values within the same range as the LTD$_4$ antagonist SKF-104353. These results suggest that these LXA$_4$ stable analogues and 15-epi-LXA$_4$ recognize the same receptors present on both neutrophils and endothelial cells as LXA$_4$.

LXA$_4$ and 15-epi-LXA$_4$ Analogues Inhibit Mouse Ear Inflammation. LXA$_4$ inhibits neutrophil adhesion and transmigration in vitro (4), and causes downregulation of CD11b/CD18 on human neutrophils (5). To evaluate this potential anti-inflammatory action of LXA$_4$ and test whether these compounds do indeed carry this action in established in vivo models, we induced skin inflammation in mouse ears and examined the impact of several new LXA$_4$ stable analogues. After topical application of LTB$_4$ on mouse ear, time-dependent increase of myeloperoxidase (MPO) activity in ear skin was observed (Fig. 8, *A–C*). Since MPO is well established as a marker of neutrophil infiltration (26), we calibrated the degree of MPO activity and the number of neutrophils using standard curves obtained from neutrophils isolated after peritoneal lavage (Fig. 8 *A*). At equimolar concentrations neither FMLP nor platelet-activating factor induced PMN infiltration when applied topically in acetone (Fig. 8 *A*). In contrast to the chemotactic ability of LTB$_4$, the same amounts of LTD$_4$ did not stimulate neutrophil infiltration into this tissue (Fig. 8 *B*).

Applied alone to the ear, 16-phenoxy-LXA$_4$ had no direct effect on neutrophil infiltration (0–8 h; Fig. 8 *B*). Also, no neutrophil influx was noted at intervals up to 48 h (not shown). When mouse ears were exposed to 16-phenoxy-LXA$_4$ just before the application of LTB$_4$, neutrophil infiltration was markedly attenuated at each time point and the percent inhibition observed at 24 h was ~85% (Fig. 8 *C*). Hematoxylin-eosin staining of ear biopsies confirmed these results and established that 16-phenoxy-LXA$_4$ applied alone did not alter the tissue architecture (Fig. 9). Ears exposed to LTB$_4$ exhibited prominent PMN infiltration in perivascular regions (*B*), and this PMN infiltration was markedly attenuated when the ear was exposed to topical 16-phenoxy-LXA$_4$ (Fig. 9 *C*).

The inhibitory action of 16-phenoxy-LXA$_4$ was concentration-dependent (Fig. 8 *D*), and an IC50 was estimated to be ~120 nmol/cm^2. When its potency was directly compared in the same model to a known anti-inflammatory agent, dexamethasone, 16-phenoxy-LXA$_4$ was as potent as dexamethasone at the equivalent concentrations (Fig. 8 *D*).

In the case of native LXA$_4$, its stereoisomer 15-epi-LXA$_4$, which is generated with aspirin treatment, carries its C-15 alcohol in the *R* configuration and is known to be more potent than native LXA$_4$ in vitro (12). To address the importance of chirality at C-15 position in vivo, we pre-

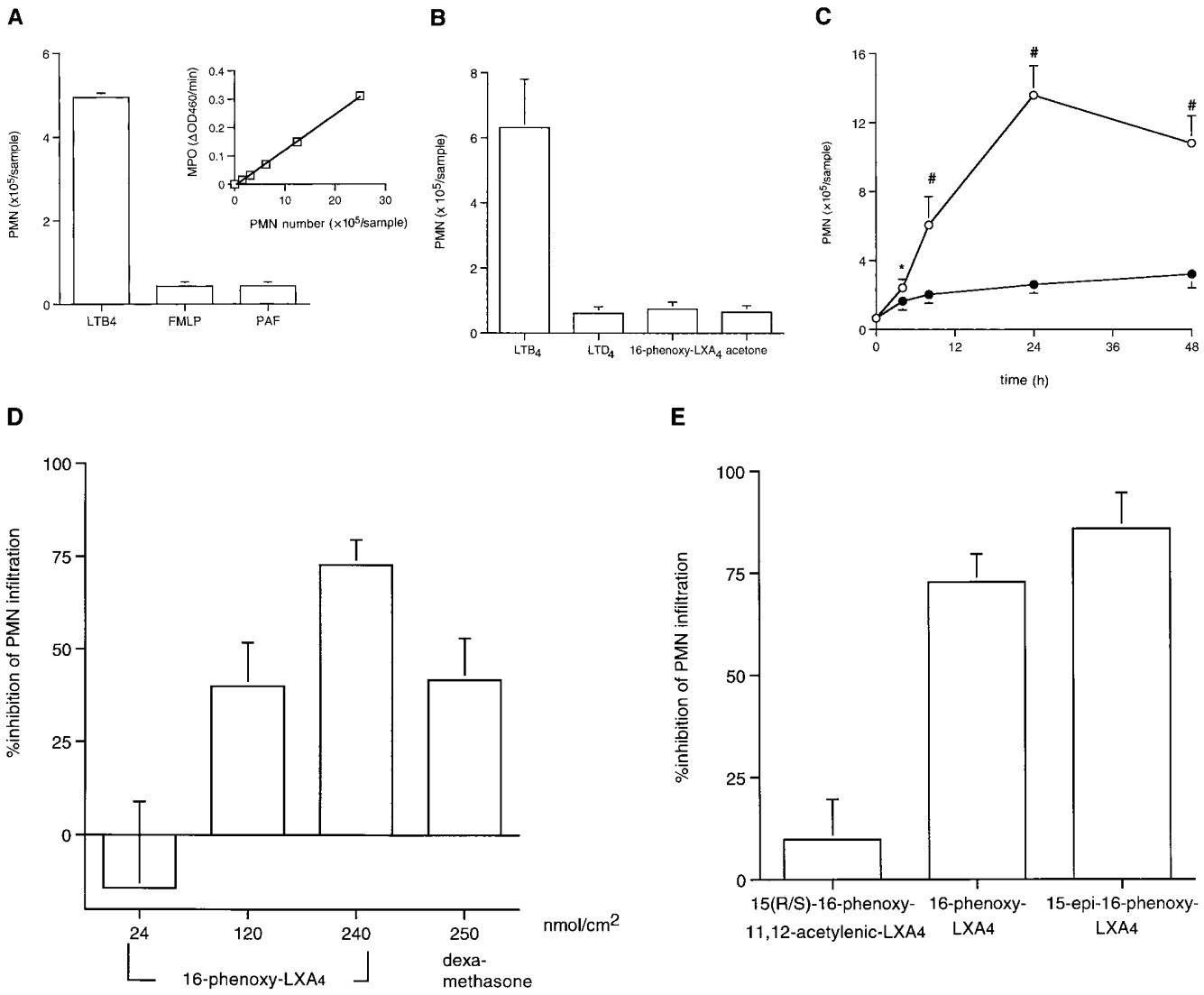

Figure 8. Topical application of LXA_4 and 15-epi-LXA_4 analogues inhibit neutrophil infiltration in vivo. (*A*) Mouse ears were topically treated with equimolar amounts of LTB_4 (1 μg), FMLP (1.3 μg), or platelet-activating factor (1.6 μg) in 20 μl of acetone. After 24 h, punch biopsy samples (6-mm diam) were obtained from each ear, and MPO activity was measured as described in Materials and Methods. MPO activity was further converted into number of neutrophils using the standard curve obtained using peritoneal neutrophils (*inset*). Neutrophils (2×10^6 cells) gave an absorbance change of 0.25 units per min at 460 nm. Results are mean ± SEM of $n = 3$–5. (*B*) Mouse ears were topically treated either with vehicle (acetone), 16-phenoxy-LXA_4 (240 nmol), LTB_4 (5 μg), or LTD_4 (5 μg). After 8 h, PMN infiltration was determined as in Fig. 8 *A*. Results are mean ± SEM of $n = 4$ (vehicle, LTB_4), $n = 3$ (LTD_4), or $n = 2$ (16-phenoxy-LXA_4). (*C*) Mouse ears were topically treated with either vehicle (○) or 16-phenoxy-LXA_4 (240 nmol) (●) and then exposed to 5 μg LTB_4 (see Materials and Methods). Results are mean ± SEM of $n = 4$. *$P < 0.01$; #, $P < 0.05$ vs. 16-phenoxy-LXA_4 treatment. (*D*) Mouse ears were topically treated either with vehicle or indicated amount of 16-phenoxy-LXA_4 or dexamethasone and then stimulated by 5 μg LTB_4 for 8 h. Percent inhibition of PMN infiltration was calculated with vehicle treated ear as 100% after background levels (MPO activity of ear treated with acetone alone) were subtracted. Results are mean ± SEM of $n = 3$ or 4. (*E*) Mouse ears were topically treated either with vehicle or 15(*R*/*S*)-16-phenoxy-11,12-acetylenic-LXA_4 (120 nmol), or 16-phenoxy-LXA_4 (240 nmol), or 15-epi-16-phenoxy-LXA_4 (240 nmol), and then exposed to LTB_4 (5 μg) for 8 h. Percent inhibition of PMN infiltration was calculated as in *D*. (Results for 16-phenoxy-LXA_4 are the same in *D*.) Results are mean ± SEM of $n = 3$–6.

pared and examined the actions of 15-epi-16-phenoxy-LXA_4 that carries its C-15 alcohol in the *R* configuration. This analogue, like 16-phenoxy-LXA_4, was designed to resist inactivation (23) and is an analogue of the aspirin-triggered 15-epi-LXA_4 from this series of LXA_4 mimetics (see Fig. 6 for structure). 15-epi-phenoxy-LXA_4 was as potent as, or more potent than, 16-phenoxy-LXA_4 (Fig. 8 *E*), a finding that supports the notion that the *R* configuration at the C-15 position augments the inhibitory actions of LXA_4 (23). When the acetylenic racemate 15(*R*/*S*)-16-phenoxy-11,12-acetylenic-LXA_4 (see Fig. 6) was examined in this model, it showed much less anti-inflammatory action than did either of the tetraene-containing compounds (i.e., 16-phenoxy-LXA_4 or 15-epi-16-phenoxy-LXA_4), suggesting that the loss of tetraene configuration abrogates bioactivity of these analogues (Fig. 8 *E*). Thus, LXA_4 and aspirin-triggered 15-epi-

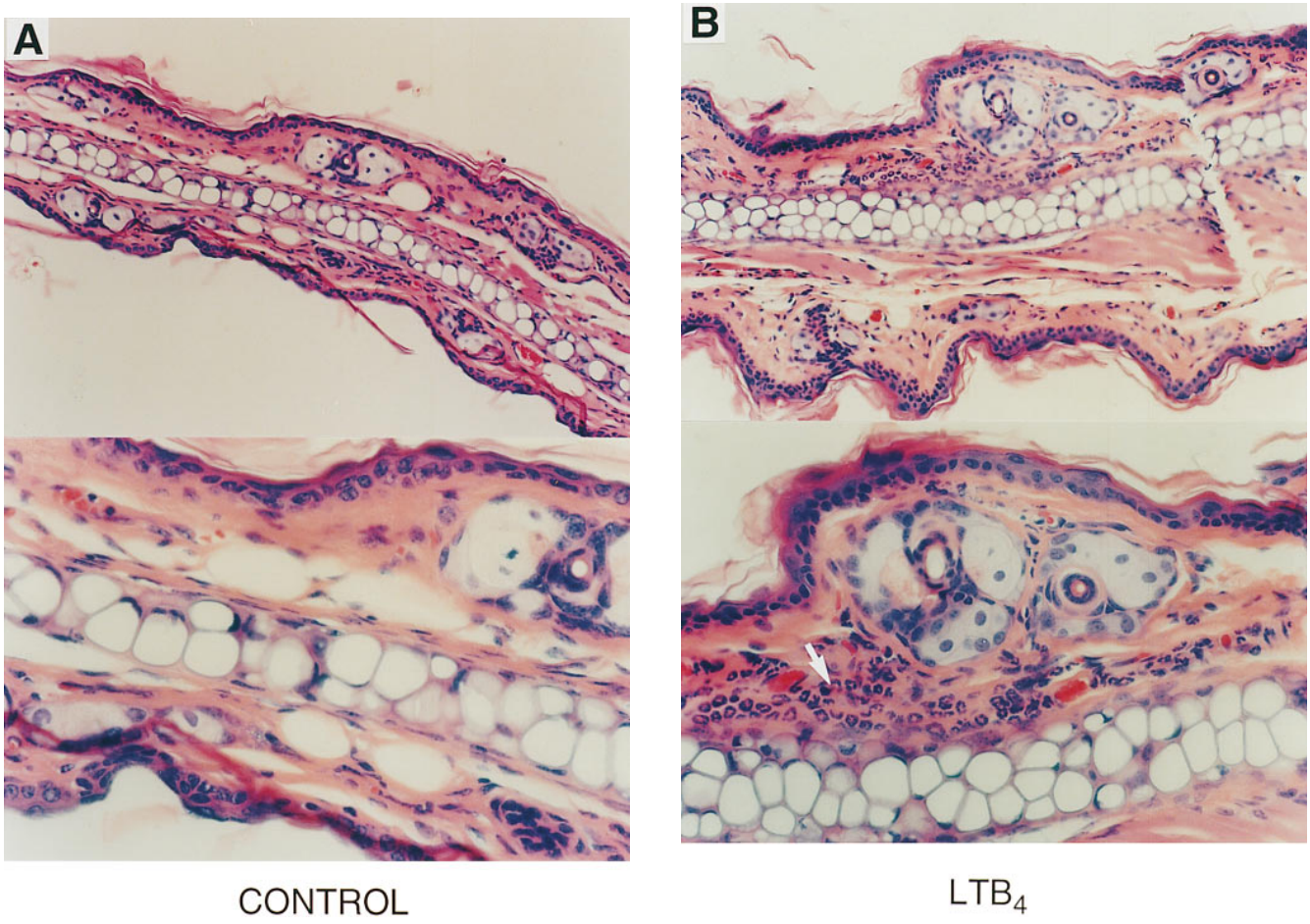

Figure 9. Ear biopsies: inhibition of LTB_4-induced neutrophil infiltration by 16-phenoxy-LXA_4. (*A*) Section of ear exposed to vehicle alone (8 h). (*B*) sections of ears exposed to LTB_4 (5 μg) for 8 h as in Fig. 8, upper panel, low power field; bottom panel, high power. Arrow indicates presence of neutrophils. (*C*) Ears exposed to 16-phenoxy-LXA_4 and LTB_4 as in Fig. 8; upper panel, low power field and bottom, high power field showing a sharp reduction in neutrophils. Sections were prepared as described in Materials and Methods and stained with hematoxylin and eosin.

LXA_4 stable analogues have anti-inflammatory actions in the mouse ear inflammation model as exemplified by inhibition of neutrophil infiltration, and this bioaction was stereoselective.

Discussion

The present results demonstrate, for the first time, cloning of the mouse myeloid LXA_4R and an anti-inflammatory action for both LXA_4 and novel aspirin-triggered LXA_4 stable analogues in vivo, namely, that topical application of these analogues and association with the murine receptor inhibits neutrophil infiltration in skin. The mouse LXA_4R isolated from a spleen cDNA library had a characteristic sequence of seven transmembrane spanning G protein–coupled receptors (27), and its homology to the human LXA_4R (6) was 73% in amino acid (Figs. 1 and 2). Mouse LXA_4R gave high-affinity binding to [^{3}H]LXA_4 (K_d 1.5 nM), with values similar to those obtained with the human LXA_4R

(1.7 nM) expressed in CHO cells (6) (Fig. 3). CHO cells stably transfected with mouse LXA_4R and exposed to LXA_4 selectively hydrolyzed GTP, indicating that LXA_4 stimulates functional coupling of LXA_4R and G protein (Fig. 4). Tissue distribution of mouse LXA_4R mRNA paralleled the appearance of human LXA_4R mRNA, and this mRNA was most abundant in mouse neutrophils, followed by spleen and lung (Fig. 5). Bioactive LXA_4 stable analogues effectively displaced both $[^3H]LXA_4$ and $[^3H]LTD_4$ binding to human neutrophils and endothelial cells, respectively (Fig. 7), results that are consistent with those obtained with native LXA_4 (18, 21). These LXA_4 analogues inhibited neutrophil infiltration in the mouse ear inflammation model, and the level of inhibition was as potent as the well established anti-inflammatory steroid, dexamethasone (Fig. 8). The inhibitory actions of LXA_4 stable analogues were stereoselective, with the *R* epimer (i.e., 15-epi-16-phenoxy-LXA_4: aspirin-triggered 15-epi-LXA_4 analogue) showing a trend for greater potency in this model (Fig. 8).

Of interest, in the phylogenetic tree, mouse and human LXA_4R belong to the chemokine receptor family, rather than having an association with other eicosanoids such as the family of prostanoid receptors (29). The leukotriene receptors remain to be identified at the molecular level. The chemokine receptor group also includes both the Fusin receptor and RANTES receptor, which have recently been shown to serve as cofactors for HIV-I infection (30, 31). LXA_4 is generated during HIV infection at least in vitro (32), but whether there is a connection between these and the present results with LXA_4 actions remains to be determined.

The results presented here are also the first direct demonstration of the ability of both LXA_4 and novel aspirin-triggered LXA_4 stable analogues to inhibit neutrophil migration in vivo. 16-phenoxy-LXA_4, which resists enzymatic degradation and is a potent inhibitor of neutrophil adhesion and transmigration in vitro (23), applied topically to mouse ear skin just before induction of inflammation clearly blocks neutrophil infiltration in a concentration-dependent fashion. LXA_4 analogue-induced inhibition of neutrophil infiltration into the ear skin was as potent as topical applications of dexamethasone and required the tetraene structure, since the 11,12-acetylenic-containing analogue was essentially not effective within this concentration range (Fig. 8). It is of particular interest to point out that other eicosanoid stable analogues such as the analogue of PGI_2, Iloprost, significantly enhance LTB_4-induced leukocyte infiltration in this mouse ear model (25). Thus the inhibitory actions of LXA_4 and 15-epi-LXA_4 stable analogues established here for the first time in an in vivo model provide evidence for the ability of LXA_4 to block neutrophil migration, which appears to be a unique action of lipoxins when compared to other eicosanoids that either initiate (i.e., LTB_4) or enhance (PGE_2, PGI_2) this response in vivo (9, 25).

These inhibitory actions of LXA_4 and 15-epi-LXA_4 analogues are not likely to be the result of blocking LTB_4 binding to its receptor on neutrophils, because LXA_4 does not compete for the specific binding of $[^3H]LTB_4$ (4°C) to neutrophils or differentiated HL-60 cells expressing LTB_4 receptors (21). One possible cellular basis for this in vivo inhibitory action of these analogues is the downregulation of neutrophil CD11b/CD18 as recently demonstrated for native LXA_4 in vitro, which requires the engagement of LXA_4R (5). Since these LXA_4 and 15-epi-LXA_4 analogues, which stereoselectively inhibit neutrophil migration, also effectively displace specific binding of $[^3H]LXA_4$ to its myeloid receptor on neutrophils (Fig. 7 *A*), it is highly likely that these LXA_4 analogues interact with the LXA_4R in vivo. This notion is supported by the finding that the mouse receptor is primarily associated with mouse neutrophils, which appear to be the target for their in vivo actions (see Results). To address a possible systemic action of the LX analogues applied topically, we added 15-epi-16-phenoxy-LXA_4 to one ear and applied LTB_4 to the other (as in Fig. 8). In this setting the LXA_4 analogue did not inhibit LTB_4-induced PMN infiltration (data not shown), suggesting that the action of these analogues was local. Along these lines, pharmacokinetic studies are in progress in this laboratory to design LX analogues with increased systemic actions. Together these findings indicate that activation of the LXA_4R in vivo results in an anti-inflammatory outcome counteracting the actions of proinflammatory signals such as LTB_4 in vivo. Moreover, they provide the first evidence for anti-inflammatory seven transmembrane spanning receptors and pathways.

Aspirin treatment of various cell types in vitro enhances native lipoxin production during cell–cell interactions and triggers the generation of 15-epi-lipoxins by a separate biosynthetic pathway (reviewed in reference 8). These novel lipoxin *R* epimers appear to mediate some of the beneficial actions of aspirin, in particular, 15-epi-LXA_4, which blocks neutrophil adhesion to endothelial cells (12). Therefore, it is of interest that 15-epi-16-phenoxy-LXA_4, an analogue of 15-epi-LXA_4, was the most potent inhibitor of neutrophil infiltration in vivo of this series of LXA_4 and 15-epi-LXA_4 analogues (Figs. 6 and 8 *E*). Aspirin has both beneficial and deleterious actions in humans. It is possible that certain of aspirin's beneficial actions might now be open to further experimentation using analogues of 15-epi-lipoxins. Taken together, the present findings provide direct further evidence that LXA_4 and novel aspirin-triggered 15-epi-LXA_4 stable analogues, as well as mouse LXA_4R cDNA, serve as useful tools to investigate the actions and role of LXA_4 and aspirin-triggered 15-epi-LXA_4 in vivo.

We thank Mary Halm Small for expert assistance in preparation of this manuscript and Dr. B. Schmidt of the Dermatopathology Division, Department of Pathology, Brigham and Women's Hospital for expert preparation and histological evaluation of the skin biopsies.

These studies were supported in part by National Institutes of Health grant nos. GM-38765 and P01-DK50305 (C.N. Serhan) and a research grant from Schering AG (C.N. Serhan and N.A. Petasis). T. Takano was also supported in part by a fellowship from the Ministry of Education, Science, and Culture of Japan.

Address correspondence to C.N. Serhan, Center for Experimental Therapeutics and Reperfusion Injury, Brigham and Women's Hospital, 75 Francis Street, Boston, MA 02115. Dr. Fiore's current address is Section of Rheumatology, University of Illinois at Chicago Medical College, Chicago, IL 60607. Dr. Brady's present address is University College Dublin, Mater Miseracordiae Hospital, Dublin, Ireland.

Received for publication 23 January 1997 and in revised form 27 February 1997.

References

1. Serhan, C.N., J.Z. Haeggström, and C.C. Leslie. 1996. Lipid mediator networks in cell signaling: update and impact of cytokines. *FASEB J.* 10:1147–1158.
2. Lee, T.H., C.E. Horton, U. Kyan-Aung, D. Haskard, A.E. Crea, and B.W. Spur. 1989. Lipoxin A_4 and lipoxin B_4 inhibit chemotactic responses of human neutrophils stimulated by leukotriene B_4 and N-formyl-L-methionyl-L-leucyl-L-phenylalanine. *Clin. Sci.* 77:195–203.
3. Colgan, S.P., C.N. Serhan, C.A. Parkos, C. Delp-Archer, and J.L. Madara. 1993. Lipoxin A_4 modulates transmigration of human neutrophils across intestinal epithelial monolayers. *J. Clin. Invest.* 92:75–82.
4. Papayianni, A., C.N. Serhan, and H.R. Brady. 1996. Lipoxin A_4 and B_4 inhibit leukotriene-stimulated interactions of human neutrophils and endothelial cells. *J. Immunol.* 156:2264–2272.
5. Fiore, S., and C.N. Serhan. 1995. Lipoxin A_4 receptor activation is distinct from that of the formyl peptide receptor in myeloid cells: inhibition of CD11/18 expression by lipoxin A_4-lipoxin A_4 receptor interaction. *Biochemistry*. 34:16678–16686.
6. Fiore, S., J.F. Maddox, H.D. Perez, and C.N. Serhan. 1994. Identification of a human cDNA encoding a functional high affinity lipoxin A_4 receptor. *J. Exp. Med.* 180:253–260.
7. Bevilacqua, M.P., R.M. Nelson, G. Mannori, and O. Cecconi. 1994. Endothelial-leukocyte adhesion molecules in human disease. *Annu. Rev. Med.* 45:361–378.
8. Serhan, C.N. 1997. Lipoxins and novel aspirin-triggered 15-epi-lipoxins (ATL): a jungle of cell-cell interactions or a therapeutic opportunity? *Prostaglandins*. 53:107–137.
9. Raud, J., U. Palmertz, S.E. Dahlén, and P. Hedqvist. 1991. Lipoxins inhibit microvascular inflammatory actions of leukotriene B_4. *Adv. Exp. Med. Biol.* 314:185–192.
10. Babior, B.M. 1994. Activation of the respiratory burst oxidase. *Environ. Health Perspect.* 102(Suppl.):53–56.
11. Nassar, G.M., J.D. Morrow, L.J. Roberts II, F.G. Lakkis, and K.F. Badr. 1994. Induction of 15-lipoxygenase by interleukin-13 in human blood monocytes. *J. Biol. Chem.* 269:27631–27634.
12. Clària, J., and C.N. Serhan. 1995. Aspirin triggers previously undescribed bioactive eicosanoids by human endothelial cell-leukocyte interactions. *Proc. Natl. Acad. Sci. USA*. 92:9475–9479.
13. Clària, J., M.H. Lee, and C.N. Serhan. 1996. Aspirin-triggered lipoxins (15-epi-LX) are generated by the human lung adenocarcinoma cell line (A549)-neutrophil interactions and are potent inhibitors of cell proliferation. *Mol. Med.* 2:583–596.
14. Kim, S.J., and T. Tominaga. 1989. Formation of lipoxins by the brain. *Ann. New York Acad. Sci.* 559:461–464.
15. Mayadas, T.N., D.L. Mendrick, H.R. Brady, T. Tang, A. Papayianni, K.J.M. Assmann, D.D. Wagner, R.O. Hynes, and R.S. Cotran. 1996. Acute passive anti-glomerular basement membrane nephritis in P-selectin-deficient mice. *Kidney Int.* 49:1342–1349.
16. Papayianni, A., C.N. Serhan, M.L. Phillips, H.G. Rennke, and H.R. Brady. 1995. Transcellular biosynthesis of lipoxin A_4 during adhesion of platelets and neutrophils in experimental immune complex glomerulonephritis. *Kidney Int.* 47:1295–1302.
17. Feng, Z., H.P. Godfrey, S. Mandy, S. Strudwick, K.-T. Lin, E. Heilman, and P.Y.-K. Wong. 1996. Leukotriene B_4 modulates *in vivo* expression of delayed-type hypersensitivity by a receptor-mediated mechanism: regulation by lipoxin A_4. *J. Pharmacol. Exp. Ther.* 278:950–956.
18. Fiore, S., S.W. Ryeom, P.F. Weller, and C.N. Serhan. 1992. Lipoxin recognition sites. Specific binding of labeled lipoxin A_4 with human neutrophils. *J. Biol. Chem.* 267:16168–16176.
19. Grandordy, B.M., H. Lacroix, E. Mavoungou, S. Krilis, A.E. Crea, B.W. Spur, and T.H. Lee. 1990. Lipoxin A_4 inhibits phosphoinositide hydrolysis in human neutrophils. *Biochem. Biophys. Res. Commun.* 167:1022–1029.
20. Badr, K.F., D.K. DeBoer, M. Schwartzberg, and C.N. Serhan. 1989. Lipoxin A_4 antagonizes cellular and in vivo actions of leukotriene D_4 in rat glomerular mesangial cells: evidence for competition at a common receptor. *Proc. Natl. Acad. Sci. USA*. 86:3438–3442.
21. Fiore, S., M. Romano, E.M. Reardon, and C.N. Serhan. 1993. Induction of functional lipoxin A_4 receptors in HL-60 cells. *Blood*. 81:3395–3403.
22. Christie, P.E., B.W. Spur, and T.H. Lee. 1992. The effects of lipoxin A_4 on airway responses in asthmatic subjects. *Am. Rev. Respir. Dis.* 145:1281–1284.
23. Serhan, C.N., J.F. Maddox, N.A. Petasis, I. Akritopoulou-Zanze, A. Papayianni, H.R. Brady, S.P. Colgan, and J.L. Madara. 1995. Design of lipoxin A_4 stable analogs that block transmigration and adhesion of human neutrophils. *Biochemistry*. 34:14609–14615.
24. Church, G.M., and W. Gilbert. 1984. Genomic sequencing. *Proc. Natl. Acad. Sci. USA*. 81:1991–1995.
25. Ekerdt, R., and B. Müller. 1992. Role of prostanoids in the inflammatory reaction and their therapeutic potential in the skin. *Arch. Dermatol. Res.* 284:S18–S21.
26. Bradley, P.P., D.A. Priebat, R.D. Christensen, and G. Rothstein. 1982. Measurement of cutaneous inflammation: estimation of neutrophil content with an enzyme marker. *J. Invest. Dermatol.* 78:206–209.
27. Strader, C.D., T.M. Fong, M.R. Tota, D. Underwood, and R.A. Dixon. 1994. Structure and function of G protein-coupled receptors. *Annu. Rev. Biochem.* 63:101–132.
28. Perez, H.D., R. Holmes, E. Kelly, J. McClary, and W.H.

Andrews. 1992. Cloning of a cDNA encoding a receptor related to the formyl peptide receptor of human neutrophils. *Gene (Amst.)*. 118:303–304.
29. Toh, H., A. Ichikawa, and S. Narumiya. 1995. Molecular evolution of receptors for eicosanoids. *FEBS Lett*. 361:17–21.
30. Feng, Y., C.C. Broder, P.E. Kennedy, and E.A. Berger. 1996. HIV-1 entry cofactor: functional cDNA cloning of a seven-transmembrane, G protein-coupled receptor. *Science (Wash. DC)*. 272:872–877.
31. Oravecz, T., M. Pall, and M.A. Norcross. 1996. β-chemokine inhibition of monocytotropic HIV-1 infection: Interference with a postbinding fusion step. *J. Immunol*. 157:1329–1332.
32. Genis, P., M. Jett, E.W. Bernton, T. Boyle, H.A. Gelbard, K. Dzenko, R.W. Keane, L. Resnick, Y. Mizrachi, D.J. Volsky et al. 1992. Cytokines and arachidonic metabolites produced during human immunodeficiency virus (HIV)-infected macrophage-astroglia interactions: implications for the neuropathogenesis of HIV disease. *J. Exp. Med*. 176:1703–1718.